Title:

Energetic Demands Regulate Sleep-Wake Rhythm Circuit Development

Authors:

Amy R. Poe[1], Lucy Zhu[1], Si Hao Tang[1], Ella Valencia[1], Matthew S. Kayser[1,2,3*]

Affiliations:

1 Department of Psychiatry, Perelman School of Medicine, University of Pennsylvania, Philadelphia, PA 19104, USA

2 Chronobiology and Sleep Institute, Perelman School of Medicine, University of Pennsylvania, Philadelphia, PA 19104, USA

3 Department of Neuroscience, Perelman School of Medicine, University of Pennsylvania, Philadelphia, PA 19104, USA

*Correspondence to: kayser@pennmedicine.upenn.edu

Abstract:

Sleep and feeding patterns lack a clear daily rhythm during early life. As diurnal animals mature, feeding is consolidated to the day and sleep to the night. Circadian sleep patterns begin with formation of a circuit connecting the central clock to arousal output neurons; emergence of circadian sleep also enables long-term memory (LTM). However, the cues that trigger the development of this clock-arousal circuit are unknown. Here, we identify a role for nutritional status in driving sleep-wake rhythm

development in *Drosophila* larvae. We find that in the 2nd instar (L2) period, sleep and feeding are spread across the day; these behaviors become organized into daily patterns by L3. Forcing mature (L3) animals to adopt immature (L2) feeding strategies disrupts sleep-wake rhythms and the ability to exhibit LTM. In addition, the development of the clock (DN1a)-arousal (Dh44) circuit itself is influenced by the larval nutritional environment. Finally, we demonstrate that larval arousal Dh44 neurons act through glucose metabolic genes to drive onset of daily sleep-wake rhythms. Together, our data suggest that changes to energetic demands in developing organisms triggers the formation of sleep-circadian circuits and behaviors.

Introduction

The development of behavioral rhythms such as sleep-wake patterns is critical for brain development[1]. Indeed, early life circadian disruptions in rodents negatively impacts adult behaviors, neuronal morphology, and circadian physiology[2-4]. Likewise, in humans, disruptions in sleep and rhythms during development are a common co-morbidity in neurodevelopmental disorders including ADHD and autism[5-8]. Although the molecular mechanisms encoding cellular rhythms are well understood, little is known about how rhythmic behaviors first emerge[1,9-11]. In particular, the possible cues that trigger the consolidation of sleep and waking behaviors as development proceeds are unclear[12-15].

A key potential factor in the maturation of sleep patterns is the coincident change in feeding and metabolism during development. Early in development, young animals must obtain enough nutrients to ensure proper growth[16]. Yet, developing organisms

47 must also sleep to support nervous system development[1]. These conflicting needs
48 (feeding vs. quiescence) result in rapid transitions between sleeping and feeding states
49 early in life. As development proceeds, nutritional intake and storage capacity increase,
50 allowing for the consolidation of feeding and sleep to specific times of day. These
51 changes in nutritional storage capacity are likely conserved as mammalian body
52 composition and nutritional capacity changes over infant development[17] and *Drosophila*
53 show rapid increases in overall larval body size including the size of the fat body (used
54 for nutrient storage) across development[18,19]. However, the role that developmental
55 changes in metabolic drive plays in regulating the consolidation of behavioral rhythms is
56 not known.

57 In adult *Drosophila*, sleep and feeding behaviors are consolidated to specific
58 times of day with flies eating more in the day than the night[20]. Yet, early in development,
59 sleep in 2nd instar *Drosophila* larvae lacks a circadian pattern[21]. We previously
60 determined that sleep-wake rhythms are initiated in early 3rd instar *Drosophila* larvae
61 (L3) (72 hr AEL). DN1a clock neurons anatomically and functionally connect to Dh44
62 arousal output neurons to drive the consolidation of sleep in L3. Development of this
63 circuit promotes deeper sleep in L3 resulting in the emergence of long-term memory
64 (LTM) capabilities at the L3 stage but not before[21].

65 Here, we identify the cues that trigger the emergence of the DN1a-Dh44 circuit
66 and the consolidation of sleep-wake rhythms in *Drosophila* larvae. We demonstrate that
67 developmental changes to energetic demands drive consolidation of periods of sleep
68 and feeding across the day as animals mature. While endogenous deeper sleep in L3
69 facilitates LTM, we find that experimentally inducing deep sleep prematurely in (L2)

70 animals is detrimental to development and does not improve LTM performance.
71 Additionally, we demonstrate that DN1a-Dh44 circuit formation is developmentally
72 plastic, as rearing on an insufficient nutritional environment prevents establishment of
73 this neural connection. Finally, we find that Dh44 neurons require glucose metabolic
74 genes to promote sleep-wake rhythm development, suggesting that these neurons
75 sense the nutritional environment to promote circadian-sleep crosstalk.
76

77 **Results**

78 *Energetic demands limit developmental onset of rhythmic behaviors*

79 The emergence of circadian sleep-wake rhythms in *Drosophila* larvae is
80 advantageous as it enables long-term memory capabilities at the L3 stage. Yet, less
81 mature larvae do not exhibit consolidated sleep-wake patterns, prompting us to ask why
82 rhythmic behaviors do not emerge earlier in life. To determine if the absence of rhythmic
83 sleep-wake patterns in L2 might be related to feeding patterns, we examined larval
84 feeding rate (# mouth hook contractions in a 5-minute period) under constant conditions
85 at 4 times across the day (Circadian Time [CT] 1, CT7, CT13, and CT19) in
86 developmentally age-matched 2nd (L2) and early 3rd instar (L3; 72 hr AEL) larvae. While
87 we observed no differences in feeding rate across the day in L2, we found that L3 show
88 diurnal differences in feeding, specifically exhibiting a higher feeding rate during the
89 subjective light times compared to the subjective dark times (Figures 1A and 1B).
90 Analysis of total overall food intake indicates that L2 feed about the same at CT1 and
91 CT13; however, L3 at CT1 feed more than L3 at CT12 (Figure S1A). To assess whether
92 the daily pattern of feeding in early L3 is dependent on the canonical circadian biological

93 clock, we examined feeding rate in null mutants for the clock gene *tim*[22]. We observed
94 no differences in feeding rate across the day in *tim* mutants indicating that daily
95 changes in feeding rate require a functioning molecular clock at the L3 stage (Figure
96 1C). These findings underscore the tight relationship between sleep and feeding across
97 development as diurnal differences in sleep emerge concurrently at the L3 stage[21].
98 To further investigate how the emergence of circadian sleep is related to
99 changes in feeding patterns during development, we asked whether enforcing a
100 constant (immature) feeding pattern at the L3 stage affects sleep-wake rhythms. First,
101 we devised a nutritional paradigm with reduced sugar content but otherwise normal food
102 (low sugar, 1.2% glucose, L.S.). Critically, this paradigm did not affect any measures of
103 larval growth or development (Figures S1D-S1F). We found that the feeding pattern in
104 L3 raised on L.S. food closely resembled that of L2 on normal food (8% glucose) with
105 feeding spread out across the day (Figure 1D) (Figure S1A). Compared to L3 raised on
106 control food, this paradigm was also associated with loss of diurnal differences in sleep
107 duration, sleep bout number, and arousal threshold (Figures 1E and 1F) (Figures S1B
108 and S1C). Next, to avoid chronic effects of this manipulation, we acutely stimulated
109 feeding in L3 reared on normal food using thermogenetic activation of NPF+ neurons
110 (Figure 2A; Figure S2A)[23,24]. Like L.S. conditions, enforcing a constant feeding pattern
111 through NPF+ neuron activation led to loss of sleep rhythms and loss of deep sleep in
112 L3 (Figures 2B-2E; Figures S2B-S2E).
113 Disruption to circadian sleep and/or to deeper sleep stages during development
114 is associated with impairments in long-term memory formation[4,25-28]. We next asked if
115 the loss of deeper sleep observed in animals adopting a constant (strategic) feeding

116 strategy through either the L.S. paradigm or NPF+ neuron activation affects long-term
117 memory (LTM) capacity. Consistent with deeper sleep stages being necessary for LTM,
118 we observed a loss of LTM in either the NPF+ neuron activation (Figure 2F; Figures
119 S2F-2I) or under L.S. conditions (Figure 2H; Figures S1G-S1I). However, short-term
120 memory (STM) was intact in both manipulations (Figures 2G and 2I). These findings
121 suggest that immature feeding strategies preclude the emergence of sleep rhythms and
122 LTM. Altogether, our data indicate that consolidated periods of sleep and feeding
123 emerge due to developmentally dynamic changes in energetic demands.
124
125 *Deeper sleep stages are energetically disadvantageous in L2*
126 To investigate if promoting deep sleep at night in L2 can enable precocious LTM
127 abilities, we fed L2 larvae the GABA-A agonist gaboxadol[29,30]. While gaboxadol feeding
128 effectively induced deeper sleep in L2 (as reflected by an increase in arousal threshold),
129 LTM was still not evident (Figures 3A and 3B, 3E; Figures S3A and S3B); however, in
130 contrast to L3, L2 on gaboxadol failed to develop normally (Figures 3C and 3D). Next, to
131 avoid chronic pharmacological manipulations altogether, we acutely stimulated sleep-
132 inducing neurons using thermogenetics. We found that activation of these neurons
133 caused an increase in sleep amount and bout length with a decrease in arousal
134 threshold (Figures 3F and 3G; Figures S3C-S3H). However, inducing deeper sleep
135 stages in L2 did not improve LTM performance (Figure 3J; Figures S3I-S3K) despite
136 STM being intact (Figure S3L). Moreover, as with gaboxadol feeding in L2,
137 thermogenetic induction of deeper sleep stages disrupted larval development (Figures
138 3H and 3I). These data suggest that sleep cannot be leveraged to enhance cognitive

139 function prematurely because prolonged periods of deep sleep are not energetically
140 sustainable at this stage.
141
142 *DN1a-Dh44 circuit formation is developmentally plastic*
143 We previously determined that Dh44 arousal neurons anatomically and
144 functionally connect to DN1a clock neurons at the L3 stage[21]. Therefore, we examined
145 the functional connectivity between clock and arousal loci in the setting of nutritional
146 perturbation by expressing ATP-gated P2X2 receptors[31] in DN1a neurons and GCaMP6
147 in Dh44 neurons. As expected, activation of DN1as in L3 raised on control food caused
148 an increase in calcium in Dh44 neurons (Figures 4A and 4B)[21]. In contrast, in L3 raised
149 on L.S. conditions, activation of DN1as no longer elicited a response in Dh44 neurons
150 (Figures 4C and 4D). Thus, the nascent connection underlying circadian sleep in
151 *Drosophila* is developmentally plastic: in an insufficient nutritional environment, this
152 connection is not functional, facilitating a more constant feeding pattern that eschews
153 deep sleep at the expense of LTM.
154 We previously determined that release of *CCHamide-1* (*CCHa1*) from DN1as to
155 *CCHa1mide-1 receptor* (*CCHa1-R*) on Dh44 neurons is necessary for sleep-wake
156 rhythms in L3[21]. Although DN1as and Dh44 are not yet connected in L2, we next asked
157 whether Dh44 neurons in L2 are competent to receive the CCHa1 signal. CCHamide-1
158 peptide was bath applied onto dissected larval brains expressing *UAS-GCaMP7* in
159 Dh44 neurons. We observed an increase in intracellular calcium in early L3 (Figure 4F);
160 however, CCHa1 application did not alter calcium levels in Dh44 neurons in L2 (Figure
161 4E), indicating that Dh44 neurons are not capable of receiving CCHa1 input prior to

162 early L3. Surprisingly, CCHa1 application in L3 raised on L.S. also failed to elicit a
163 response in Dh44 neurons (Figure 4G) raising the possibility that sub-optimal nutritional
164 milieu influences the development of Dh44 neuronal competency to receive clock-driven
165 cues. Altogether, our data suggest that the nutritional environment influences DN1a-
166 Dh44 circuit development.
167
168 *Dh44 neurons require glucose metabolic genes to regulate sleep-wake rhythms*
169 How do developing larvae detect changes in their nutritional environments to
170 drive the circadian consolidation of sleep and feeding at the L3 stage? In adult
171 *Drosophila*, Dh44 neurons act as nutrient sensors to regulate food consumption and
172 starvation-induced sleep suppression through the activity of both glucose and amino
173 acid sensing genes[32-35]. We next asked whether Dh44 neurons in L3 require metabolic
174 genes to regulate sleep-wake rhythms. We conducted an RNAi-based candidate screen
175 in L3 raised on control food of different glucose and amino acid sensing genes known to
176 act in adult Dh44 neurons. Sleep duration at CT1 and CT13 was assessed with
177 knockdown of glucose metabolic genes (*Hexokinase-C*, *Glucose transporter 1,* and
178 *Pyruvate kinase*) or amino acid sensing genes (*Gcn2* and its downstream target ATF4
179 or *cryptocephal*) in Dh44 neurons. We found that knockdown of glucose metabolism
180 genes, *Glut1*, *Hex-C* and *PyK*, in Dh44 neurons resulted in a loss of rhythmic changes
181 in sleep duration and bout number (Figures 5A-5C; Figures S4A-S4F) with no effect on
182 L3 feeding in the *Hex-C* manipulation (Figure 5D). Manipulation of glucose metabolic
183 genes in L2 did not affect sleep duration at CT1 and CT13 (Figures 5E-5G; Figures
184 S4G-S4L) providing evidence that nutrient sensing is not required at this stage to

185 regulate sleep. In contrast to their role in adult Dh44 neurons, knockdown of amino acid
186 sensing genes, *Gcn2* and *crc*, in Dh44 neurons did not disrupt rhythmic changes in
187 sleep duration and bout number in L3 (Figures 5H and 5I; Figures S4M-S4P)
188 suggesting that Dh44 neurons may not act through amino acid sensing pathways to
189 regulate sleep-wake rhythm development. Thus, Dh44 neurons require glucose
190 metabolic genes to drive sleep-wake rhythm development. Our data indicate that the
191 emergence of diurnal behavioral differences such as sleep-wake is driven by
192 developmental changes in energetic capacity and suggest that Dh44 neurons may be
193 necessary for sensing of larval nutritional environments.
194

195 **Discussion**

196 Nutritional environment and energetic status exert profound effects on sleep
197 patterns during development, but mechanisms coupling sleep to these factors remain
198 undefined. We report that the development of sleep-circadian circuits depends on
199 organisms achieving sufficient nutritional status to support the consolidation of deep
200 sleep at night. In contrast to their role in adult flies, our data demonstrate that larval
201 Dh44 neurons act through glucose metabolic genes but not amino acid sensing genes
202 to modulate sleep-wake rhythms. This suggests that larval Dh44 neurons may have
203 distinct functions from their adult counterparts for integrating information about the
204 nutritional environment through the direct sensing of glucose levels to modulate sleep-
205 wake rhythm development. Maintaining energy homeostasis and sensing of the
206 nutritional environment are likely conserved regulators of sleep-wake rhythm

207 development as young mice exposed to a maternal low-protein diet show disruptions in
208 night-time sleep architecture and energy expenditure later in life[36,37].
209 Together with our previously published work, our findings support a model in
210 which changes in both overall circuit development and molecular changes in post-
211 synaptic (Dh44) neurons likely drive sleep-wake rhythm circuit development. Our
212 CCHa1 peptide data suggest that Dh44 neurons may undergo changes in CCHa1-R
213 expression or subcellular localization between the L2 and L3 stages; we only observed
214 an increase in Dh44 neural activity in response to the bath application of CCHa1
215 peptide at the L3 stage (Figures 4E and 4F). Interestingly, this increase in activity is lost
216 in low nutrient conditions (Figure 4G) suggesting that the larval nutritional environment
217 may also modulate CCHa1-R localization or expression. Indeed, we observed a
218 disruption of sleep rhythms in L3 when glucose metabolic genes are knocked down in
219 Dh44 neurons demonstrating that post-synaptic changes likely initiate onset of circadian
220 sleep. These findings raise intriguing questions for how changes in an organism's
221 energetic and nutritional state influence sleep-circadian circuit development. Perhaps
222 larval Dh44 neurons respond to an increase in glucose levels in the environment by
223 promoting CCHa1-R localization to the membrane. In this model, changes in CCHa1-R
224 subcellular localization allow Dh44 neurons to become competent to receive clock-
225 driven cues, while this or other Dh44-derived signals promote circuit connectivity with
226 DN1as to drive consolidation of sleep at the L3 stage. There are no available
227 endogenous fluorescent reporters of CCHa1-R, limiting our ability to examine receptor
228 subcellular localization. Nevertheless, our data provide exciting avenues of future work

229 on the molecular and subcellular mechanisms regulating DN1a-Dh44 circuit
230 development.

231 Our data demonstrate that larvae exhibit both sleep-wake and feeding rhythms at
232 the L3 stage, but not earlier[21]. This raises the obvious question of whether sleep and
233 feeding are opposite sides of the same coin. While larvae cannot eat when they are
234 sleeping, we have observed distinct effects of certain manipulations on sleep behaviors
235 but not feeding. For example, knockdown of *Hex-C* in Dh44 neurons disrupts sleep
236 rhythms with no obvious effect on feeding behavior (Figure 5D). Moreover, preliminary
237 data suggests that manipulating possible feeding-rhythmic relevant circuitry disrupts
238 feeding rhythms with no apparent effect on sleep-wake rhythms (data not shown). It is,
239 of course, possible to affect both sleep and feeding behaviors with the same circuit
240 manipulation indicating that they are also inter-connected behaviors. For example,
241 thermogenetic activation of NPF+ neurons causes an increase in feeding rate while also
242 causing a decrease in sleep duration. Future work will leverage the larval system to
243 examine how sleep-wake and feeding circuitry communicate to balance these two
244 behaviors across developmental periods.
245

246 **Acknowledgements:**
247 We thank members of the Kayser Lab, Raizen Lab, David Raizen, and other members
248 of the Penn Chronobiology and Sleep Institute for helpful discussions and input.
249

250 **Funding:**

This work was supported by NIH DP2NS111996 and a Burroughs Wellcome Career Award for Medical Scientists to M.S.K.; NIH T32HL007713 and a Hartwell Foundation Fellowship to A.R.P.

Author contributions:

Conceptualization, A.R.P., M.S.K.; Investigation, A.R.P., L.Z., S.H.T., E.V.; Writing – Original Draft, A.R.P. and M.S.K.; Writing – Review & Editing, all authors; Project supervision and funding, M.S.K.

Data and Materials Availability: All data needed to evaluate the conclusions in the paper are present in the paper and/or the Supplementary Materials.

Competing Interests: All authors declare that they have no competing interests.

Materials and Methods

Fly Stocks

The following lines have been maintained as lab stocks or were obtained from Dr. Amita Sehgal: iso31, tim0[22], Dh44^{VT}-Gal4 (VT039046)[38], cry-Gal4 pdf-Gal80[39], UAS-TrpA1[40], UAS-mCherry RNAi, LexAOP-GCaMP6 UAS-P2X2[31], and UAS-GCaMP7f. Dh44-LexA (80703), npf-Gal4 (25681), R76G11-Gal4 (48333), Hex-C RNAi (57404), Glut1 RNAi (40904), PyK RNAi (35218), GCN2 RNAi (67215), and crc RNAi (80388) were from the Bloomington *Drosophila* Stock Center (BDSC).

274 **Larval rearing and sleep assays**

275 Larval sleep experiments were performed as described previously[21,41]. Briefly, molting
276 2nd instar or 3rd instar larvae were placed into individual wells of the LarvaLodge
277 containing either 120 µl (for L2) or 95 µl (for L3) of 3% agar and 2% sucrose media
278 covered with a thin layer of yeast paste. The LarvaLodge was covered with a
279 transparent acrylic sheet and placed into a DigiTherm (Tritech Research) incubator at
280 25°C for imaging. Experiments were performed in the dark. For thermogenetic
281 experiments, adult flies were maintained at 22°C. Larvae were then placed into the
282 LarvaLodge (as described above) which was moved into a DigiTherm (Tritech
283 Research) incubator at 30°C for imaging.

284

285 **LarvaLodge image acquisition and processing**

286

287 Images were acquired every 6 seconds with an Imaging Source DMK 23GP031 camera
288 (2592 X 1944 pixels, The Imaging Source, USA) equipped with a Fujinon lens
289 (HF12.55A-1, 1:1.4/12.5 mm, Fujifilm Corp., Japan) with a Hoya 49mm R72 Infrared
290 Filter as described previously[21,41]. We used IC Capture (The Imaging Source) to acquire
291 time-lapse images. All experiments were carried out in the dark using infrared LED
292 strips (Ledlightsworld LTD, 850 nm wavelength) positioned below the LarvaLodge.
293 Images were analyzed using custom-written MATLAB software (see Churgin et al
294 2019[42] and Szuperak et al 2018[41]). Temporally adjacent images were subtracted to
295 generate maps of pixel value intensity change. A binary threshold was set such that
296 individual pixel intensity changes that fell below 40 gray-scale units within each well

297 were set equal to zero (“no change”) to eliminate noise. For 3rd instars, the threshold
298 was set to 45 to account for larger body size. Pixel changes greater than or equal to
299 threshold value were set equal to one (“change”). Activity was then calculated by taking
300 the sum of all pixels changed between images. Sleep was defined as an activity value
301 of zero between frames. For 2nd instar sleep experiments done across the day, total
302 sleep was summed over 6 hrs beginning 2 hrs after the molt to second instar. For sleep
303 experiments performed at certain circadian times, total sleep in the 2nd hour after the
304 molt to second (or third) instar was summed.
305
306 **Feeding behavior analysis**
307 For feeding rate analysis, newly molted 2nd instar or 3rd instar larvae were placed in
308 individual wells of the LarvaLodge containing 120 µl of 3% agar and 2% sucrose media
309 covered with a thin layer of yeast paste. Larvae were then imaged continuously with a
310 Sony HDR-CX405 HD Handycam camera (B&H Photo, Cat. No: SOHDRCX405) for 5
311 minutes. The number of mouth hook contractions (feeding rate) was counted manually
312 over the imaging period and raw numbers were recorded. For food intake analysis,
313 newly molted 2nd instar or 3rd instar larvae were starved for 1 hr in petri dishes with
314 water placed on a Kimwipe. To compare groups of larvae of similar body weights, 13 L3
315 larvae and 26 L2 larvae were grouped together. Larvae were placed in a petri dish
316 containing blue-dyed 3% agar, 2% sucrose, and 2.5% apple juice with blue-dyed yeast
317 paste on top for 4 hrs at 25°C in constant darkness. After 4 hrs, groups of larvae were
318 washed in water, put in microtubes, and frozen at -80°C for 1 hr. Frozen larvae were
319 then homogenized in 300 µl of distilled water and spun down for 5 min at 13,0000 rpm.

320 The amount of blue dye in the supernatant was then measured using a
321 spectrophotometer (OD_{629}). Food intake represents the OD value of each
322 measurement.
323
324 **Aversive Olfactory conditioning**
325 We used an established two odor reciprocal olfactory conditioning paradigm with 10 mM
326 quinine (quinine hydrochloride, EMSCO/Fisher, Cat. No: 18-613-007) as a negative
327 reinforcement to test short-term or long-term memory performance in L2 and early L3
328 larvae[43] at CT12-15[21]. Experiments were conducted on assay plates (100 X 15 mm,
329 Genesee Scientific, Cat. No: 32-107) filled with a thin layer of 2.5% agarose containing
330 either pure agarose (EMSCO/Fisher, Cat. No: 16500-500) or agarose plus reinforcer.
331 As olfactory stimuli, we used 10 μl amyl acetate (AM, Sigma-Aldrich, Cat. No:
332 STBF2370V, diluted 1:50 in paraffin oil-Sigma-Aldrich, Cat. No: SZBF140V) and octanol
333 (OCT, Fisher Scientific, Cat. No: SALP564726, undiluted). Odorants were loaded into
334 the caps of 0.6 mL tubes (EMSCO/Fisher, Cat. No: 05-408-123) and covered with
335 parafilm (EMSCO/Fisher, Cat. No: 1337412). For naïve preferences of odorants, a
336 single odorant was placed on one side of an agarose plate with no odorant on the other
337 side. A group of 30 larvae were placed in the middle. After 5 minutes, individuals were
338 counted on the odorant side, the non-odorant side, or in the middle. The naïve
339 preference was calculated by subtracting the number of larvae on the non-odorant side
340 from the number of larvae on the odorant side and then dividing by the total number of
341 larvae. For naïve preference of quinine, a group of 30 larvae were placed in the middle
342 of a half agarose-half quinine plate. After 5 minutes, individuals were counted on the

343 quinine side, the agarose side, or in the middle. The naïve preference for quinine was
344 calculated by subtracting the number of larvae on the quinine side from the number of
345 larvae on the agarose side and then dividing by the total number of larvae. Larvae were
346 trained by exposing a group of 30 larvae to AM while crawling on agarose medium plus
347 quinine reinforcer. After 5 min, larvae were transferred to a fresh Petri dish containing
348 agarose alone with OCT as an odorant (AM+/OCT). A second group of 30 larvae
349 received the reciprocal training (AM/OCT+). Three training cycles were used for all
350 experiments. For long-term memory, larvae were transferred after training onto agarose
351 plates with a small piece of Kimwipe moistened with tap water and covered in dry active
352 yeast (LabScientific, Cat. No: FLY804020F). Larvae were then kept in the dark for 1.5
353 hrs before testing memory performance. Training and retention for thermogenetic
354 experiments were conducted at 30°C. For short-term memory, larvae were immediately
355 transferred after training onto test plates (agarose plus reinforcer) on which AM and
356 OCT were presented on opposite sides of the plate. After 5 min, individuals were
357 counted on the AM side, the OCT side, or in the middle. We then calculated a
358 preference index (PREF) for each training group by subtracting the number of larvae on
359 the conditioned stimulus side from the number of larvae on the unconditioned stimulus
360 side. For one set of experiments, we calculated two PREF values: 1a) $PREF_{AM+/OCT}$ =
361 (#AM - #OCT)/ # TOTAL; 1b) $PREF_{AM/OCT+}$ = (#OCT-#AM)/ # TOTAL. We then took the
362 average of each PREF value to calculate an associative performance index (PI) as a
363 measure of associative learning. PI = ($PREF_{AM+/OCT}$ + $PREF_{AM/OCT+}$)/2.
364

365 **Arousal threshold**

366 Blue light stimulation was delivered as described in [21,41] using 2 high power LEDs
367 (Luminus Phatlight PT-121, 460 nm peak wavelength, Sunnyvale, CA) secured to an
368 aluminum heat sink. The LEDs were driven at a current of 0.1 A (low intensity). We
369 used a low intensity stimulus for 4 sec every 2 minutes for 1 hr beginning the 2nd hr after
370 the molt to second (or third) instar. We then counted the number of larvae that showed
371 an activity change in response to stimulus. The percentage of animals that moved in
372 response to the stimulus was recorded for each experiment. For each genotype, at least
373 4 biological replicates were performed. We then plotted the average percentage across
374 all replicates.
375
376 **P2X2 Activation and GCaMP imaging**
377 All live imaging experiments (P2X2 and CCHa1 bath application) were performed as
378 described previously[21]. Briefly, brains were dissected in artificial hemolymph (AHL)
379 buffer consisting of (in mM): 108 NaCl, 5 KCl, 2 CaCl2, 8.2 MgCl2, 4 NaHCO3, 1
380 NaH2PO4-H20, 5 Trehalose, 10 Sucrose, 5 HEPES, pH=7.5. Brains were placed on a
381 small glass coverslip (Carolina Cover Glasses, Circles, 12 mm, Cat. No: 633029) in a
382 perfusion chamber filled with AHL.
383 For P2X2 imaging, dissections were performed at CT12-15 and AHL buffer was
384 perfused over the brains for 1 min of baseline GCaMP6 imaging, then ATP was
385 delivered to the chamber by switching the perfusion flow from the channel containing
386 AHL to the channel containing 2.5 mM ATP in AHL, pH 7.5. ATP was perfused for 2 min
387 and then AHL was perfused for 2 min. Twelve-bit images were acquired with a 40 X
388 water immersion objective at 256 X 256-pixel resolution. Z-stacks were acquired every 5

389 sec for 3 min. Image processing and measurement of fluorescence intensity was
390 performed in ImageJ as described previously[21]. For each cell body, fluorescence traces
391 over time were normalized using this equation: $\Delta F/F = (F_n - F_0)/F_0$, where
392 F_n=fluorescence intensity recorded at time point n, and F_0 is the average fluorescence
393 value during the 1 min baseline recording. Maximum GCaMP change ($\Delta F/F$) for
394 individual cells was calculated using this equation: $\Delta F/F_{max} = (F_{max} - F_0)/F_0$, where
395 F_{max}=maximum fluorescence intensity value recorded during ATP application, and F_0 is
396 the average fluorescence value during the 1 min baseline recording. All analysis was
397 done blind to experimental condition.
398 For CCHa1 bath application, dissections were performed at CT12-15 and AHL
399 buffer was perfused over the brains for 1 min of baseline GCaMP7f imaging, then
400 CCHa1 peptide was delivered to the chamber by switching the perfusion flow from the
401 channel containing AHL to the channel containing 1 μM synthetic CCHa1 in AHL, pH
402 7.5. CCHa1 was perfused for 2 min, followed by a 1 min wash-out with AHL. For the
403 AHL negative control, the perfusion flow was switched from one channel containing AHL
404 to another channel containing AHL. Twelve-bit images were acquired with a 40 X water
405 immersion objective at 256 X 256-pixel resolution. Z-stacks were acquired every 10 sec
406 for 4 min. Image processing and measurement of fluorescence intensity was performed
407 in ImageJ. A max intensity Z-projection of each time step and Smooth thresholding was
408 used for analysis. Image analysis was performed in a similar manner as for the P2X2
409 experiments. All analysis was done blind to experimental condition.
410
411 **Gaboxadol treatment**

412 Early second or third instar larvae were starved for 1 hour and then fed 75 µl of 25
413 mg/mL Gaboxadol (hydrochloride) (Thomas Scientific, Cat No: C817P41) in diluted
414 yeast solution for 1 hour prior to loading in LarvaLodge containing 120 µl of 3% agar
415 and 2% sucrose media covered with a thin layer of 25 mg/mL Gaboxadol yeast paste.
416 For LTM experiments, starved early second instars were fed 25 mg/mL Gaboxadol for 1
417 hour prior to training and maintained on 25 mg/mL Gaboxadol in diluted yeast solution
418 during retention period.
419
420 **Dietary Manipulations**
421 Fly food was prepared using the following recipes (based on Poe et al 2020)[44]:

Ingredients	Control food (444 mM glucose)	Low sugar (L.S.) (66 mM glucose)
Distilled H_2O	234 mL	234 mL
Agar	2 g (10g/L)	2 g (10g/L)
Glucose	20 g	3 g
Inactive yeast	20 g	20 g
Acid mix (phosphoric acid + propionic acid)	2 mL	2 mL
Target final solution volume	250 mL	250 mL

422

423 Acid Mix was made by preparing Solution A (41.5 ml Phosphoric Acid mixed with 458.5
424 ml distilled water) and Solution B (418 ml Propionic Acid mixed with 82 ml distilled
425 water) separately and then mixing Solution A and Solution B together.
426 Adult flies were placed in an embryo collection cage (Genesee Scientific, cat#: 59-100)
427 and eggs were laid on a petri dish containing either control (ctrl) or Low sugar (L.S.)
428 food. Animals developed on this media for three days.
429
430 **Larval Body Weight and Length Measurements**
431 For weight, groups of 5 early 3rd instar larvae raised on either control- or low sugar
432 (L.S.)-filled petri dishes were washed in tap water and dried using a Kimwipe. The 5
433 larvae were then weighed as a group on a scale and the weight in mg was recorded.
434 For the Gaboxadol experiments, groups of 10 early 2nd instar larvae or groups of 5 early
435 3rd instar larvae were weighed. For length, images of individual early 3rd instar larvae in
436 the LarvaLodge were measured in ImageJ (Fiji) using the straight line tool. The total
437 body length was determined in pixels for individual larvae on each condition.
438
439 **Statistical analysis**
440 All statistical analysis was done in GraphPad (Prism). For comparisons between 2
441 conditions, two-tailed unpaired *t*-tests were used. For comparisons between multiple
442 groups, ordinary one-way ANOVAs followed by Tukey's multiple comparison tests were
443 used. For comparisons between different groups in the same analysis, ordinary one-
444 way ANOVAs followed by Sidak's multiple comparisons tests were used. For
445 comparisons between time and genotype, two-way ANOVAs followed by Sidak's

446 multiple comparisons tests were used. For comparison of GCaMP signal in CCHa1

447 experiments, Mann-Whitney test was used. *P<0.05, **P<0.01, ***P<0.001.

448 Representative confocal images are shown from at least 8-10 independent samples

449 examined in each case.

450

451 **References**

452 1. Vallone, D., Lahiri, K., Dickmeis, T., and Foulkes, N.S. (2007). Start the clock!
453 Circadian rhythms and development. Dev Dyn *236*, 142-155. 10.1002/dvdy.20998.
454 2. Varcoe, T.J., Voultsios, A., Gatford, K.L., and Kennaway, D.J. (2016). The impact of
455 prenatal circadian rhythm disruption on pregnancy outcomes and long-term metabolic
456 health of mice progeny. Chronobiol Int *33*, 1171-1181.
457 10.1080/07420528.2016.1207661.
458 3. Mendez, N., Halabi, D., Spichiger, C., Salazar, E.R., Vergara, K., Alonso-Vasquez, P.,
459 Carmona, P., Sarmiento, J.M., Richter, H.G., Seron-Ferre, M., and Torres-Farfan, C.
460 (2016). Gestational Chronodisruption Impairs Circadian Physiology in Rat Male
461 Offspring, Increasing the Risk of Chronic Disease. Endocrinology *157*, 4654-4668.
462 10.1210/en.2016-1282.
463 4. Ameen, R.W., Warshawski, A., Fu, L., and Antle, M.C. (2022). Early life circadian
464 rhythm disruption in mice alters brain and behavior in adulthood. Sci Rep *12*, 7366.
465 10.1038/s41598-022-11335-0.
466 5. Hoffmire, C.A., Magyar, C.I., Connolly, H.V., Fernandez, I.D., and van Wijngaarden, E.
467 (2014). High prevalence of sleep disorders and associated comorbidities in a community
468 sample of children with Down syndrome. J Clin Sleep Med *10*, 411-419.
469 10.5664/jcsm.3618.
470 6. Krakowiak, P., Goodlin-Jones, B., Hertz-Picciotto, I., Croen, L.A., and Hansen, R.L.
471 (2008). Sleep problems in children with autism spectrum disorders, developmental
472 delays, and typical development: a population-based study. J Sleep Res *17*, 197-206.
473 10.1111/j.1365-2869.2008.00650.x.
474 7. Kotagal, S. (2015). Sleep in Neurodevelopmental and Neurodegenerative Disorders.
475 Semin Pediatr Neurol *22*, 126-129. 10.1016/j.spen.2015.03.003.
476 8. Ednick, M., Cohen, A.P., McPhail, G.L., Beebe, D., Simakajornboon, N., and Amin, R.S.
477 (2009). A review of the effects of sleep during the first year of life on cognitive,
478 psychomotor, and temperament development. Sleep *32*, 1449-1458.
479 10.1093/sleep/32.11.1449.
480 9. Carmona-Alcocer, V., Abel, J.H., Sun, T.C., Petzold, L.R., Doyle, F.J., 3rd, Simms, C.L.,
481 and Herzog, E.D. (2018). Ontogeny of Circadian Rhythms and Synchrony in the
482 Suprachiasmatic Nucleus. J Neurosci *38*, 1326-1334. 10.1523/JNEUROSCI.2006-
483 17.2017.

10. Sehgal, A., Price, J., and Young, M.W. (1992). Ontogeny of a biological clock in Drosophila melanogaster. Proc Natl Acad Sci U S A *89*, 1423-1427. 10.1073/pnas.89.4.1423.
11. Poe, A.R., Mace, K.D., and Kayser, M.S. (2021). Getting into rhythm: developmental emergence of circadian clocks and behaviors. FEBS J. 10.1111/febs.16157.
12. Blumberg, M.S., Seelke, A.M., Lowen, S.B., and Karlsson, K.A. (2005). Dynamics of sleep-wake cyclicity in developing rats. Proc Natl Acad Sci U S A *102*, 14860-14864. 10.1073/pnas.0506340102.
13. Blumberg, M.S., Gall, A.J., and Todd, W.D. (2014). The development of sleep-wake rhythms and the search for elemental circuits in the infant brain. Behav Neurosci *128*, 250-263. 10.1037/a0035891.
14. Frank, M.G., Ruby, N.F., Heller, H.C., and Franken, P. (2017). Development of Circadian Sleep Regulation in the Rat: A Longitudinal Study Under Constant Conditions. Sleep *40*. 10.1093/sleep/zsw077.
15. Frank, M.G. (2020). The Ontogenesis of Mammalian Sleep: Form and Function. Curr Sleep Med Rep *6*, 267-279. 10.1007/s40675-020-00190-y.
16. Ghosh, S., Korte, A., Serafini, G., Yadav, V., and Rodenfels, J. (2023). Developmental energetics: Energy expenditure, budgets and metabolism during animal embryogenesis. Semin Cell Dev Biol *138*, 83-93. 10.1016/j.semcdb.2022.03.009.
17. Toro-Ramos, T., Paley, C., Pi-Sunyer, F.X., and Gallagher, D. (2015). Body composition during fetal development and infancy through the age of 5 years. Eur J Clin Nutr *69*, 1279-1289. 10.1038/ejcn.2015.117.
18. Butterworth, F.M., Emerson, L., and Rasch, E.M. (1988). Maturation and degeneration of the fat body in the Drosophila larva and pupa as revealed by morphometric analysis. Tissue Cell *20*, 255-268. 10.1016/0040-8166(88)90047-x.
19. Jacobs, H.T., George, J., and Kemppainen, E. (2020). Regulation of growth in Drosophila melanogaster: the roles of mitochondrial metabolism. J Biochem *167*, 267-277. 10.1093/jb/mvaa002.
20. Barber, A.F., Erion, R., Holmes, T.C., and Sehgal, A. (2016). Circadian and feeding cues integrate to drive rhythms of physiology in Drosophila insulin-producing cells. Genes Dev *30*, 2596-2606. 10.1101/gad.288258.116.
21. Poe, A.R., Zhu, L., Szuperak, M., McClanahan, P.D., Anafi, R.C., Scholl, B., Thum, A.S., Cavanaugh, D.J., and Kayser, M.S. (2023). Developmental emergence of sleep rhythms enables long-term memory in Drosophila. Sci Adv *9*, eadh2301. 10.1126/sciadv.adh2301.
22. Konopka, R.J., and Benzer, S. (1971). Clock mutants of Drosophila melanogaster. Proc Natl Acad Sci U S A *68*, 2112-2116. 10.1073/pnas.68.9.2112.
23. Wu, Q., Wen, T., Lee, G., Park, J.H., Cai, H.N., and Shen, P. (2003). Developmental Control of Foraging and Social Behavior by the Drosophila Neuropeptide Y-like System. Neuron *39*, 147-161. 10.1016/s0896-6273(03)00396-9.
24. Chung, B.Y., Ro, J., Hutter, S.A., Miller, K.M., Guduguntla, L.S., Kondo, S., and Pletcher, S.D. (2017). Drosophila Neuropeptide F Signaling Independently Regulates Feeding and Sleep-Wake Behavior. Cell Rep *19*, 2441-2450. 10.1016/j.celrep.2017.05.085.

25. Konrad, C., Seehagen, S., Schneider, S., and Herbert, J.S. (2016). Naps promote flexible memory retrieval in 12-month-old infants. Dev Psychobiol *58*, 866-874. 10.1002/dev.21431.
26. Seehagen, S., Konrad, C., Herbert, J.S., and Schneider, S. (2015). Timely sleep facilitates declarative memory consolidation in infants. Proc Natl Acad Sci U S A *112*, 1625-1629. 10.1073/pnas.1414000112.
27. Jones, C.E., Opel, R.A., Kaiser, M.E., Chau, A.Q., Quintana, J.R., Nipper, M.A., Finn, D.A., Hammock, E.A.D., and Lim, M.M. (2019). Early-life sleep disruption increases parvalbumin in primary somatosensory cortex and impairs social bonding in prairie voles. Sci Adv *5*, eaav5188. 10.1126/sciadv.aav5188.
28. Smarr, B.L., Grant, A.D., Perez, L., Zucker, I., and Kriegsfeld, L.J. (2017). Maternal and Early-Life Circadian Disruption Have Long-Lasting Negative Consequences on Offspring Development and Adult Behavior in Mice. Sci Rep *7*, 3326. 10.1038/s41598-017-03406-4.
29. Dissel, S., Angadi, V., Kirszenblat, L., Suzuki, Y., Donlea, J., Klose, M., Koch, Z., English, D., Winsky-Sommerer, R., van Swinderen, B., and Shaw, P.J. (2015). Sleep restores behavioral plasticity to Drosophila mutants. Curr Biol *25*, 1270-1281. 10.1016/j.cub.2015.03.027.
30. Dijk, D.J., Stanley, N., Lundahl, J., Groeger, J.A., Legters, A., Trap Huusom, A.K., and Deacon, S. (2012). Enhanced slow wave sleep and improved sleep maintenance after gaboxadol administration during seven nights of exposure to a traffic noise model of transient insomnia. J Psychopharmacol *26*, 1096-1107. 10.1177/0269881111421971.
31. Yao, Z., Macara, A.M., Lelito, K.R., Minosyan, T.Y., and Shafer, O.T. (2012). Analysis of functional neuronal connectivity in the Drosophila brain. J Neurophysiol *108*, 684-696. 10.1152/jn.00110.2012.
32. Dus, M., Lai, J.S., Gunapala, K.M., Min, S., Tayler, T.D., Hergarden, A.C., Geraud, E., Joseph, C.M., and Suh, G.S. (2015). Nutrient Sensor in the Brain Directs the Action of the Brain-Gut Axis in Drosophila. Neuron *87*, 139-151. 10.1016/j.neuron.2015.05.032.
33. Yang, Z., Huang, R., Fu, X., Wang, G., Qi, W., Mao, D., Shi, Z., Shen, W.L., and Wang, L. (2018). A post-ingestive amino acid sensor promotes food consumption in Drosophila. Cell Res *28*, 1013-1025. 10.1038/s41422-018-0084-9.
34. Oh, Y., Lai, J.S., Min, S., Huang, H.W., Liberles, S.D., Ryoo, H.D., and Suh, G.S.B. (2021). Periphery signals generated by Piezo-mediated stomach stretch and Neuromedin-mediated glucose load regulate the Drosophila brain nutrient sensor. Neuron *109*, 1979-1995 e1976. 10.1016/j.neuron.2021.04.028.
35. Oh, Y., and Suh, G.S.B. (2023). Starvation-induced sleep suppression requires the Drosophila brain nutrient sensor. J Neurogenet, 1-8. 10.1080/01677063.2023.2203489.
36. Sutton, G.M., Centanni, A.V., and Butler, A.A. (2010). Protein malnutrition during pregnancy in C57BL/6J mice results in offspring with altered circadian physiology before obesity. Endocrinology *151*, 1570-1580. 10.1210/en.2009-1133.
37. Crossland, R.F., Balasa, A., Ramakrishnan, R., Mahadevan, S.K., Fiorotto, M.L., and Van den Veyver, I.B. (2017). Chronic Maternal Low-Protein Diet in Mice Affects Anxiety, Night-Time Energy Expenditure and Sleep Patterns, but Not Circadian Rhythm in Male Offspring. PLoS One *12*, e0170127. 10.1371/journal.pone.0170127.

572 38. Jenett, A., Rubin, G.M., Ngo, T.T., Shepherd, D., Murphy, C., Dionne, H., Pfeiffer, B.D.,
573 Cavallaro, A., Hall, D., Jeter, J., et al. (2012). A GAL4-driver line resource for
574 Drosophila neurobiology. Cell Rep *2*, 991-1001. 10.1016/j.celrep.2012.09.011.
575 39. Stoleru, D., Peng, Y., Agosto, J., and Rosbash, M. (2004). Coupled oscillators control
576 morning and evening locomotor behaviour of Drosophila. Nature *431*, 862-868.
577 10.1038/nature02926.
578 40. Hamada, F.N., Rosenzweig, M., Kang, K., Pulver, S.R., Ghezzi, A., Jegla, T.J., and
579 Garrity, P.A. (2008). An internal thermal sensor controlling temperature preference in
580 Drosophila. Nature *454*, 217-220. 10.1038/nature07001.
581 41. Szuperak, M., Churgin, M.A., Borja, A.J., Raizen, D.M., Fang-Yen, C., and Kayser, M.S.
582 (2018). A sleep state in Drosophila larvae required for neural stem cell proliferation.
583 eLife *7*. 10.7554/eLife.33220.
584 42. Churgin, M.A., Szuperak, M., Davis, K.C., Raizen, D.M., Fang-Yen, C., and Kayser,
585 M.S. (2019). Quantitative imaging of sleep behavior in Caenorhabditis elegans and larval
586 Drosophila melanogaster. Nat Protoc *14*, 1455-1488. 10.1038/s41596-019-0146-6.
587 43. Widmann, A., Artinger, M., Biesinger, L., Boepple, K., Peters, C., Schlechter, J., Selcho,
588 M., and Thum, A.S. (2016). Genetic Dissection of Aversive Associative Olfactory
589 Learning and Memory in Drosophila Larvae. PLoS Genet *12*, e1006378.
590 10.1371/journal.pgen.1006378.
591 44. Poe, A.R., Xu, Y., Zhang, C., Lei, J., Li, K., Labib, D., and Han, C. (2020). Low FoxO
592 expression in Drosophila somatosensory neurons protects dendrite growth under nutrient
593 restriction. Elife *9*. 10.7554/eLife.53351.
594

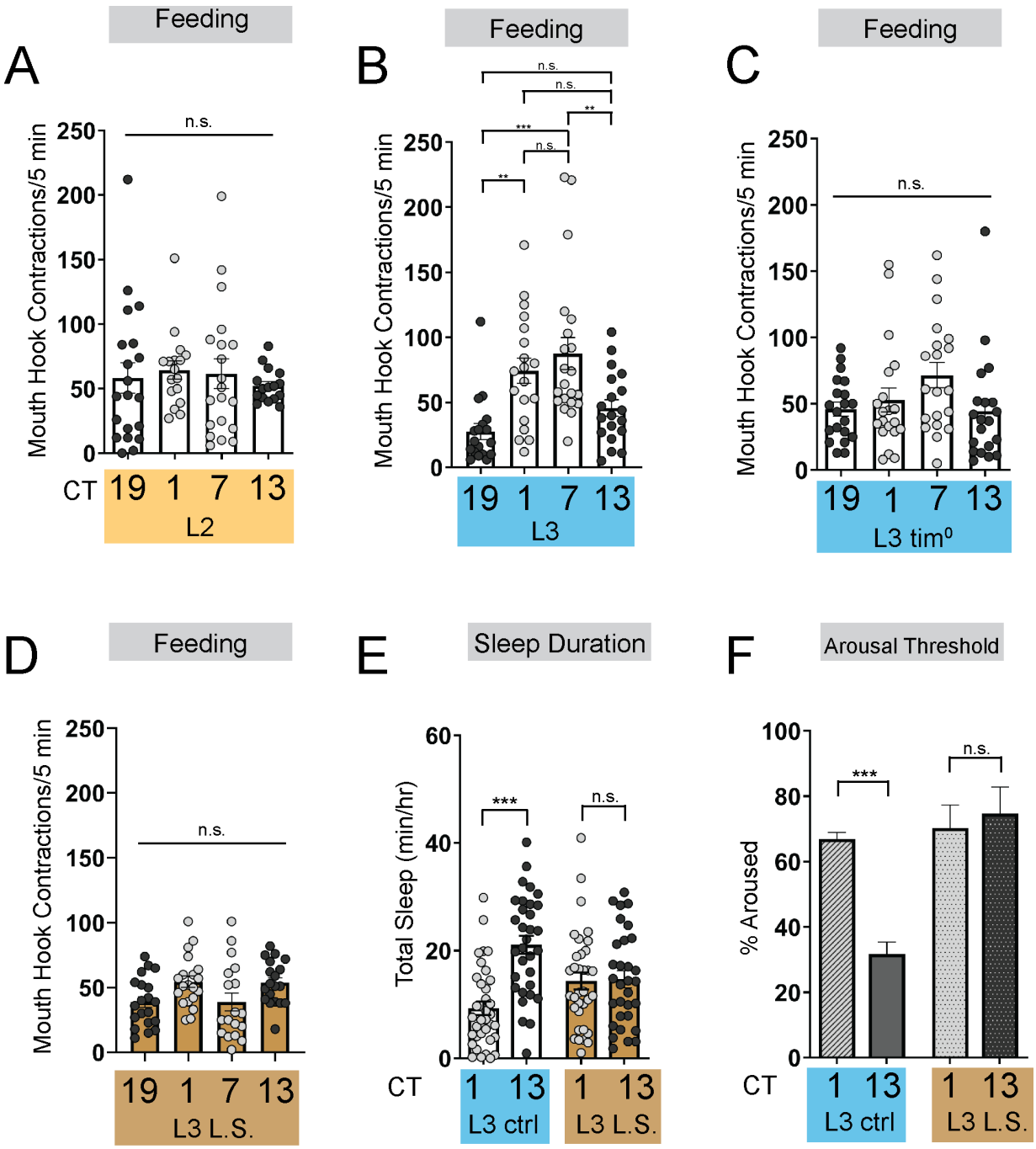

Figure 1: Energetic drive limits sleep rhythm development
(A-D) Feeding rate (# of mouth hook contractions per 5 min) of L2 controls (A), L3 raised on regular (ctrl) food (B), L3 clock mutants (C), and L3 raised on low sugar (L.S.) food (D) across the day. **(E)** Sleep duration at CT1 and CT13 in L3 raised on regular (ctrl) and L.S. food. **(F)** Arousal threshold at CT1 and CT13 in L3 raised on regular (ctrl) and L.S. food. A-D, n=18-20 larvae; E, n=29-34 larvae; F, n= n=100-172 sleep episodes, 18 larvae per genotype**.** One-way ANOVAs followed by Sidak's multiple comparisons tests [(A-D)]; Two-way ANOVAs followed by Sidak's multiple comparison test [(E-F)]. For

this and all other figures unless otherwise specified, data are presented as mean ± SEM; n.s., not significant, *$P<0.05$, **$P<0.01$, ***$P<0.001$.

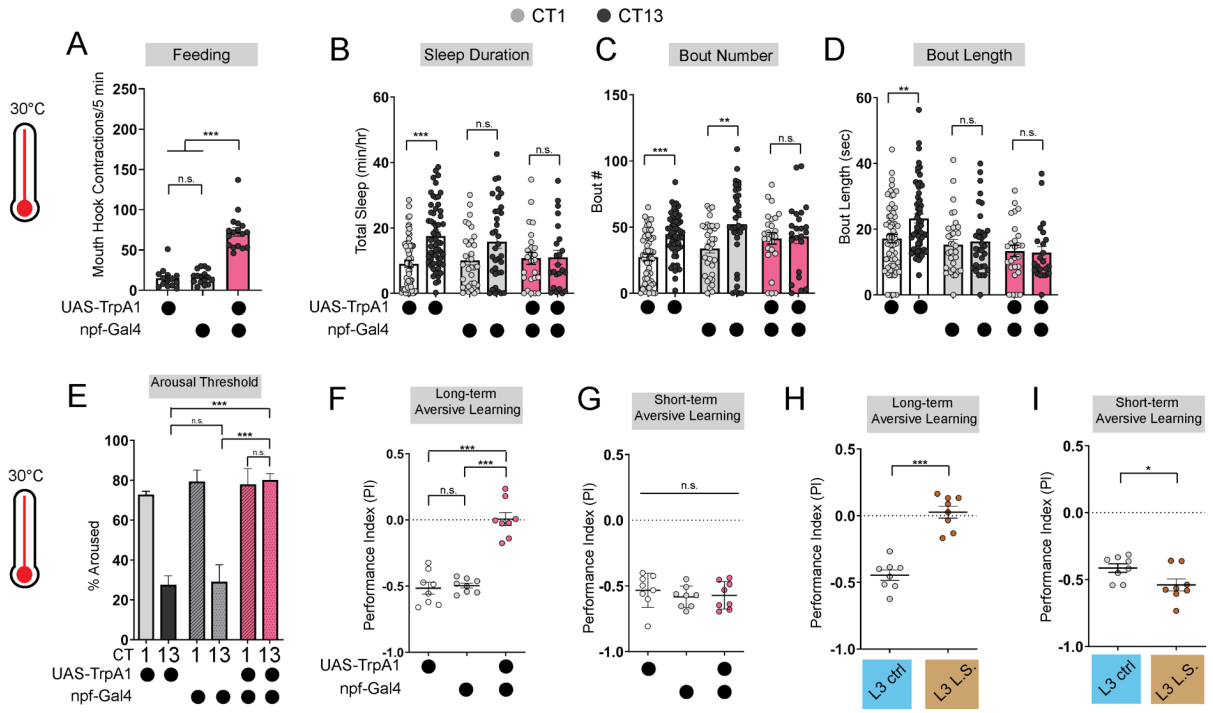

Figure 2: Immature feeding strategies perturb LTM performance.
(A) Feeding rate of L3 expressing *npf*-Gal4>*UAS-TrpA1* and genetic controls at 30°C at CT13. **(B-D)** Sleep duration (B), bout number (C), and bout length (D) of L3 expressing *npf*-Gal4>*UAS-TrpA1* and genetic controls at 30°C. **(E-G)** Arousal threshold (E), long-term aversive memory performance (F), and short-term aversive memory performance (G) in L3 expressing *npf*-Gal4>*UAS-TrpA1* and genetic controls at 30°C. **(H,I)** Short-and long-term term aversive memory performance in L3 raised on ctrl and L.S. food. A, n=18-20 larvae; B-D, n=24-61 larvae; E, n=125-160 sleep episodes, 18 larvae per genotype; F-I, n=8 PIs (240 larvae) per genotype. One-way ANOVAs followed by Sidak's multiple comparisons tests [(A) and (E-G)]; Two-way ANOVAs followed by Sidak's multiple comparison test [(B-D)]; unpaired two-tailed Student's *t*-test [(H) and (I)].

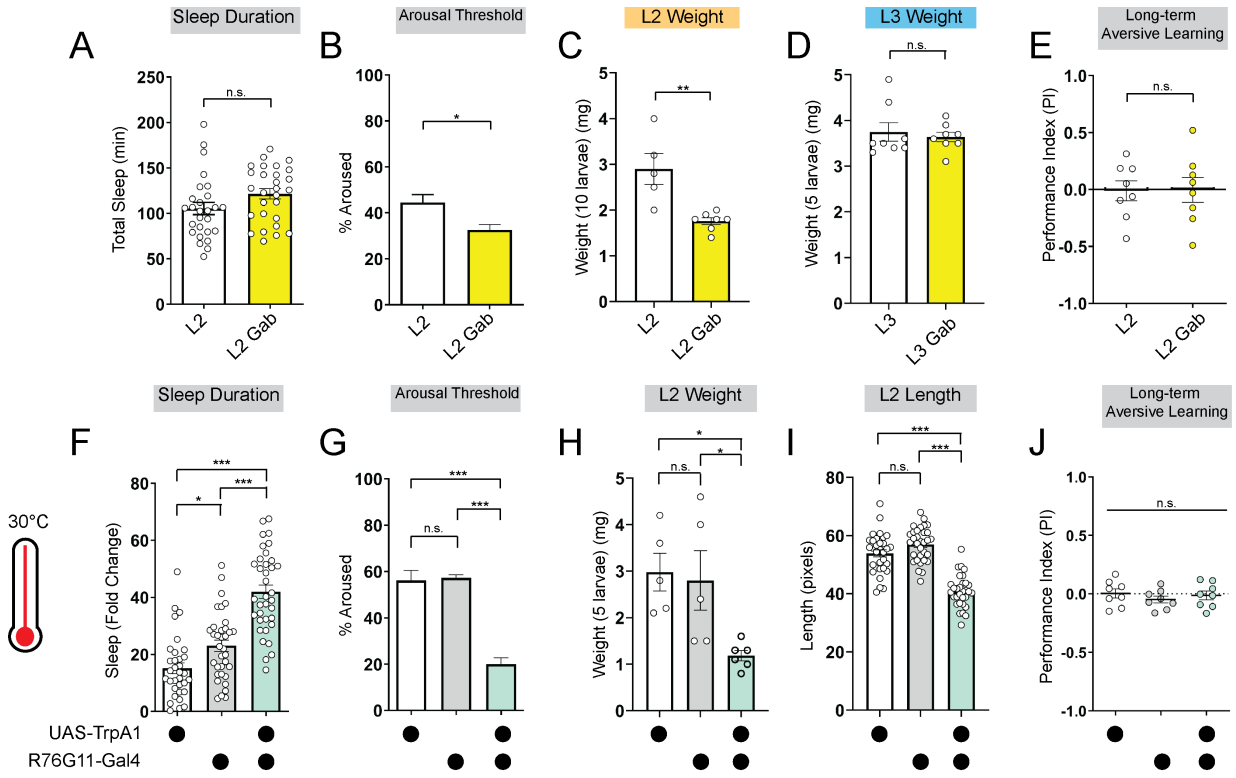

Figure 3: Deeper sleep stages in L2 are energetically disadvantageous.
(A, B) Sleep duration (A) and arousal threshold (B) of L2 control fed vehicle control (L2) or Gaboxadol (L2 Gab). **(C, D)** Total body weight of L2 (C) (in groups of 10) or L3 (D) (in groups of 5) fed vehicle control or Gaboxadol (Gab). **(E)** Long-term aversive memory performance in L2 fed vehicle control (L2) or Gaboxadol (L2 Gab). **(F, G)** Sleep duration (F) and arousal threshold (G) of L2 expressing *R76G11*-Gal4>*UAS-TrpA1* and genetic controls at 30°C. **(H, I)** Total body weight (H) and total body length (I) of L2 expressing *R76G11*-Gal4>*UAS-TrpA1* and genetic controls at 30°C. **(J)** Long-term aversive memory performance of L2 expressing *R76G11*-Gal4>*UAS-TrpA1* and genetic controls at 30°C. A, n=28 larvae; B, n=110-220 sleep episodes, 18 larvae per genotype; C, n=5-7 groups (50-70 larvae); D, n=8 groups (40 larvae); E, n=8 PIs (240 larvae) per genotype; F, n=33-36 larvae; G, n=234-404 sleep episodes, 30-40 larvae per genotype; H, n=5 groups (25 larvae); I, n=31-32 larvae; J, n=8 PIs (240 larvae) per genotype. Unpaired two-tailed Student's *t*-tests [(A-E)]; one-way ANOVAs followed by Sidak's multiple comparisons tests [(F-J)].

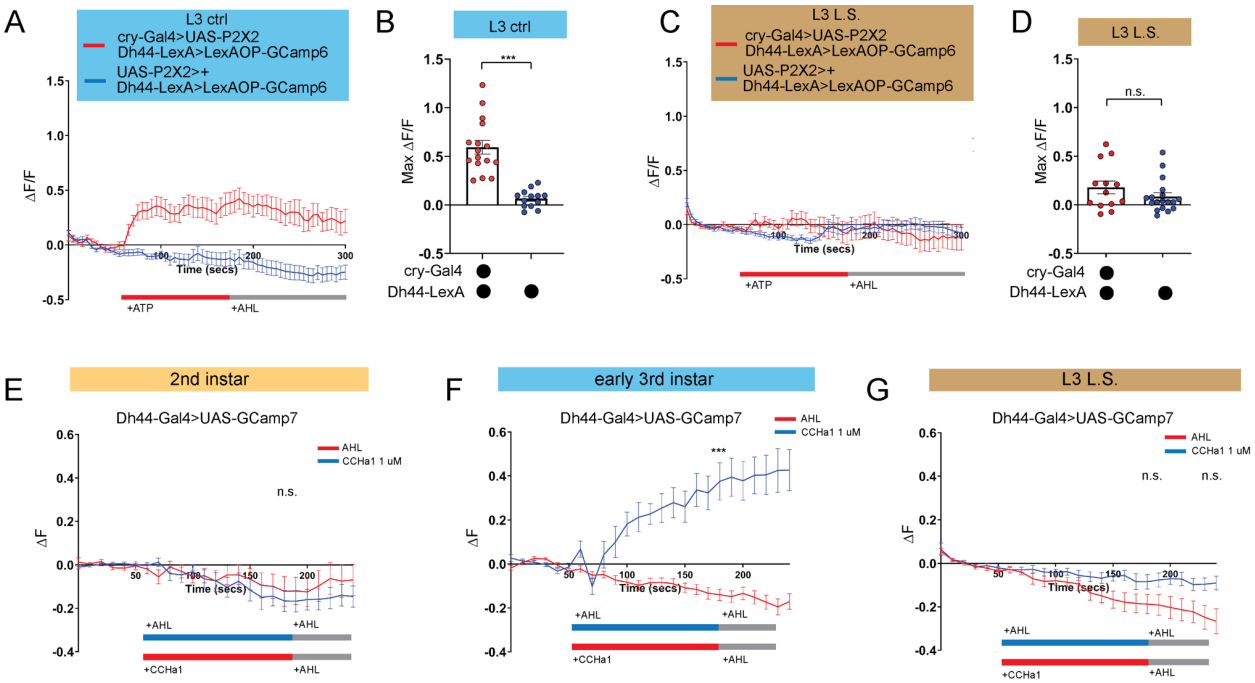

Figure 4: DN1a-Dh44 circuit formation is developmentally plastic.
(A, C) GCaMP6 signal in Dh44 neurons with activation of DN1a neurons in L3 controls (A) and L3 raised on L.S. food (C). Red bar indicates ATP application and gray bar indicates AHL application. **(B, D)** Maximum GCaMP change (ΔF/F) for individual cells in L3 controls (B) and L3 raised on L.S. food (D). **(E-G)** GCaMP7 signal in Dh44 neurons during bath application of 1 μM CCHa1 synthetic peptide in L2 (E), L3 controls (F) and L3 raised on L.S. food (G) brains. Red/blue bar indicates timing of CCHa1 (red) or buffer (AHL, blue) application and gray bar indicates timing of washout AHL application. A-D, n=12-18 cells, 8-10 brains; E-G, n=11-15 cells, 5-10 brains. Unpaired two-tailed Student's *t*-tests [(B) and (D)]; Mann-Whitney U test [(E-G)].

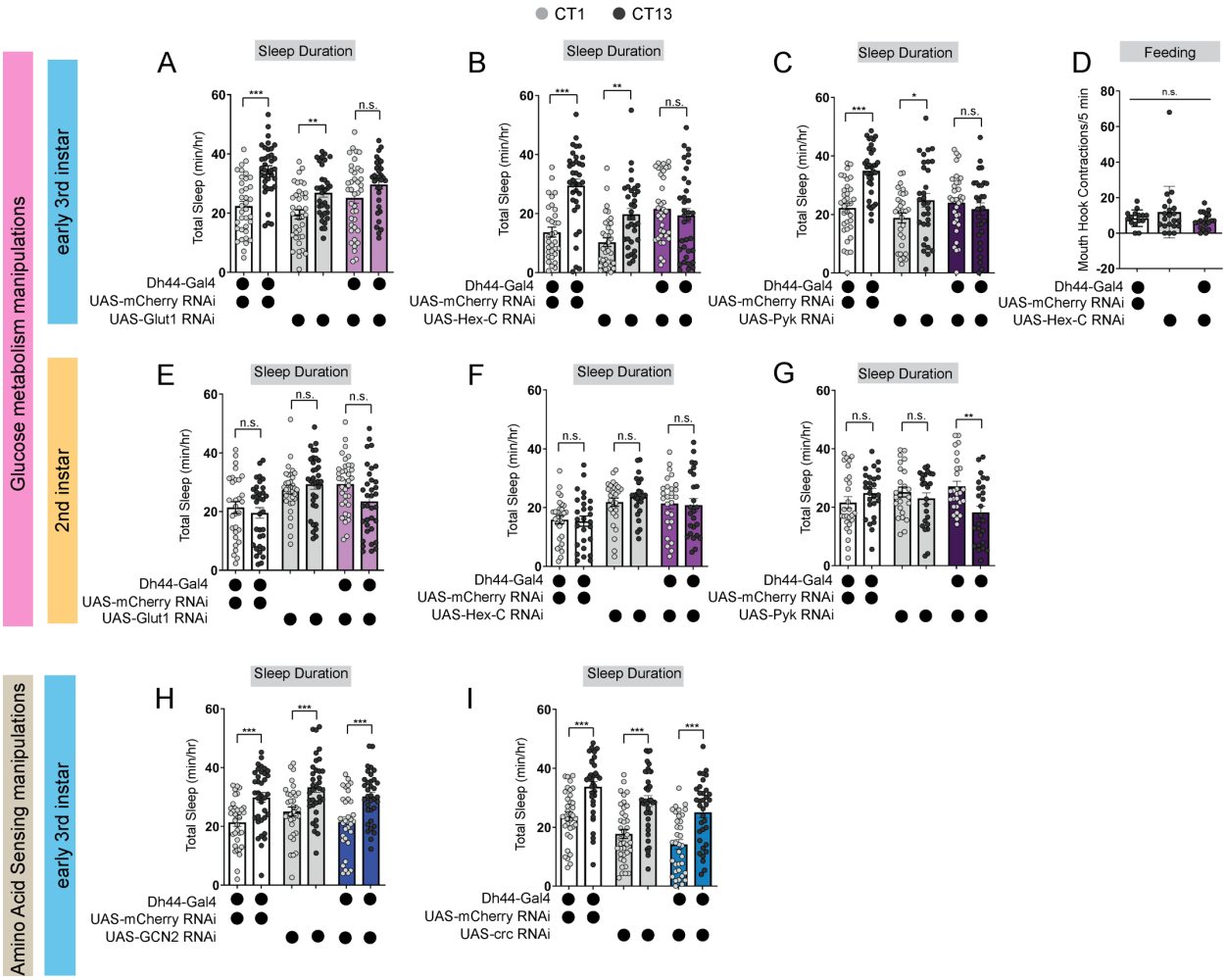

Figure 5: Dh44 neurons require glucose metabolic genes in L3 to regulate sleep-wake rhythms.

(A-C) Sleep duration in L3 expressing *UAS-Glut1-RNAi* (A), *UAS-Hex-C-RNAi* (B), and *UAS-Pyk-RNAi* (C) with *Dh44-Gal4* and genetic controls at CT1 and CT13. **(D)** Feeding rate (# of mouth hook contractions per 5 min) of L3 expressing *UAS-Hex-C-RNAi* with *Dh44-Gal4* and genetic controls at CT13. **(E-G)** Sleep duration in L2 expressing *UAS-Glut1-RNAi* (E), *UAS-Hex-C-RNAi* (F), and *UAS-Pyk-RNAi* (G) with *Dh44-Gal4* and genetic controls at CT1 and CT13. **(H, I)** Sleep duration in L3 expressing *UAS-GCN2-RNAi* (H) and *UAS-crc-RNAi* (I) with *Dh44-Gal4* and genetic controls at CT1 and CT13. A-C, n=32-40 larvae; D, n=20 larvae; E-I, n=32-40 larvae. Two-way ANOVAs followed by Sidak's multiple comparison test [(A-C) and (E-I)]; One-way ANOVAs followed by Sidak's multiple comparisons tests [(D)].

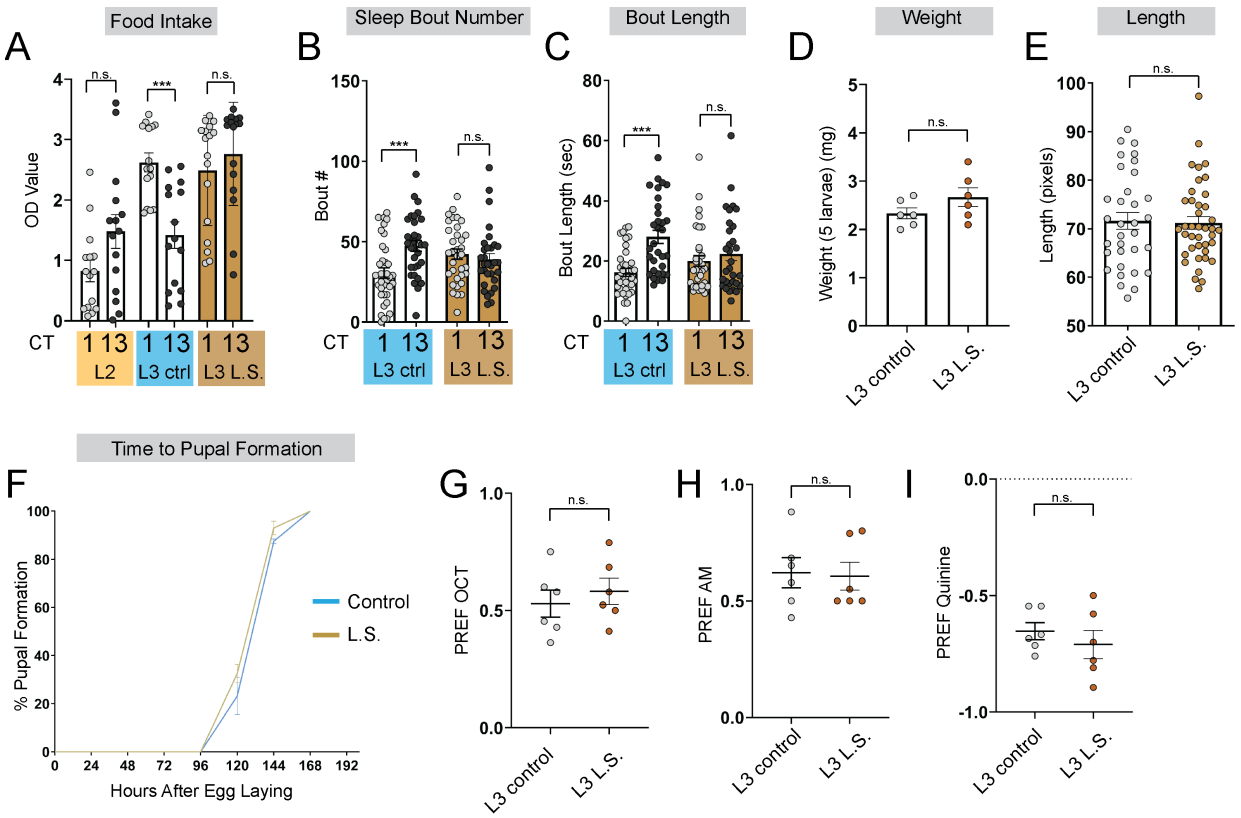

Supplemental Figure 1: Larvae on low sugar diets develop normally.
(A) Feeding amount of L2 controls, L3 raised on regular (ctrl) food, and L3 raised on low sugar (L.S.) food at CT1 and CT13. **(B, C)** Sleep bout number (B) and bout length (C) at CT1 and CT13 in L3 raised on regular (ctrl) and L.S. food. **(D)** Total body weight of early L3 (in groups of 5) raised on ctrl or L.S. food. **(E)** Total body length of early L3 raised on ctrl or L.S. food. **(F)** Developmental analysis of time to pupal formation of animals raised on ctrl or L.S. food. **(G-I)** Naïve OCT, AM, and quinine preference in L3 raised on ctrl and L.S. food. B-C, n=29-34 larvae; D, n=30 larvae per food condition; E, n=33-40 larvae; F, n=100-170 larvae; G-I, n=6 PREFs (180 larvae) per genotype. Two-way ANOVAs followed by Sidak's multiple comparison test [(B-C)]; Unpaired two-tailed Student's *t*-tests [(D-E) and (G-I)].

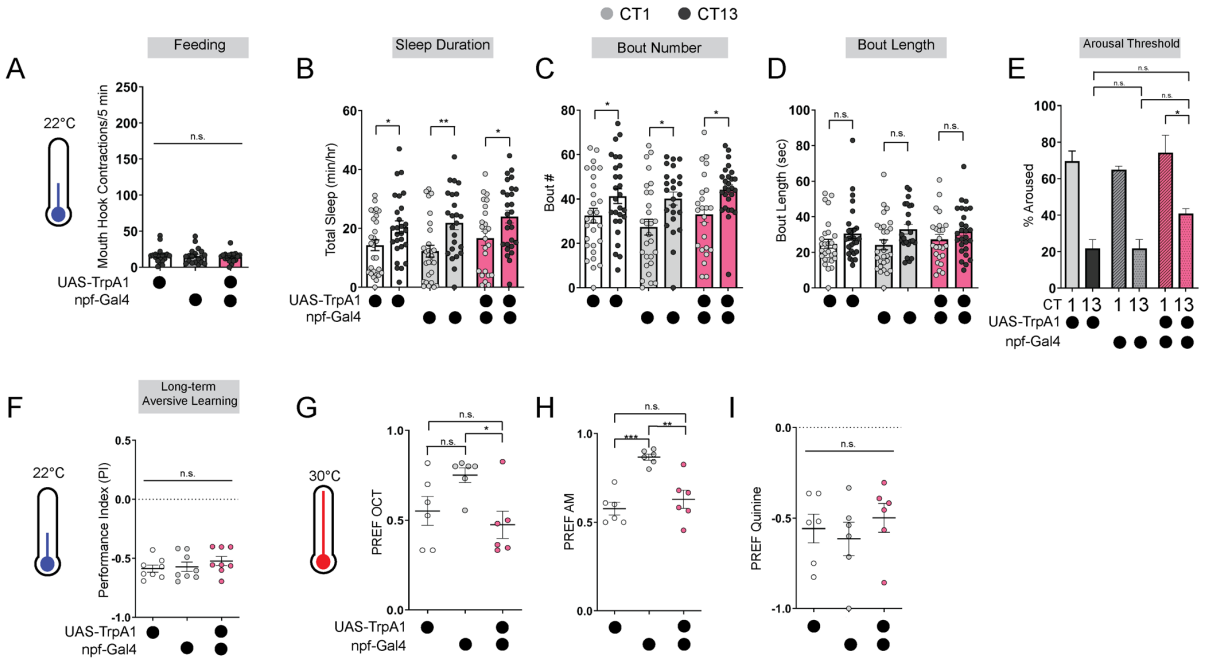

Supplemental Figure 2: Baseline odor preferences, feeding, and sleep are not affected by *npf*-Gal4 manipulations.

(A) Feeding rate of L3 expressing *npf*-Gal4>*UAS-TrpA1* and genetic controls at 22°C at CT13. **(B-E)** Sleep duration (B), bout number (C), bout length (D), and arousal threshold (E) in L3 expressing *npf*-Gal4>*UAS-TrpA1* and genetic controls at CT1 and CT13 at 22°C (temperature controls). **(F)** Long-term aversive memory performance in L3 expressing *npf*-Gal4>*UAS-TrpA1* and genetic controls at 22°C (temperature controls). **(G-I)** Naïve OCT, AM, and quinine preference in L3 expressing *npf*-Gal4>*UAS-TrpA1* and genetic controls at 30°C. A, n=18-20 larvae; B-D, n=22-27 larvae; E, n=120-205 sleep episodes, 18 larvae per genotype; F, n=8 PIs (240 larvae) per genotype; G-I, n=6 PREFs (180 larvae) per genotype. One-way ANOVAs followed by Sidak's multiple comparisons tests [(A), (E), and (F-I)]; Two-way ANOVAs followed by Sidak's multiple comparison test [(B-D)].

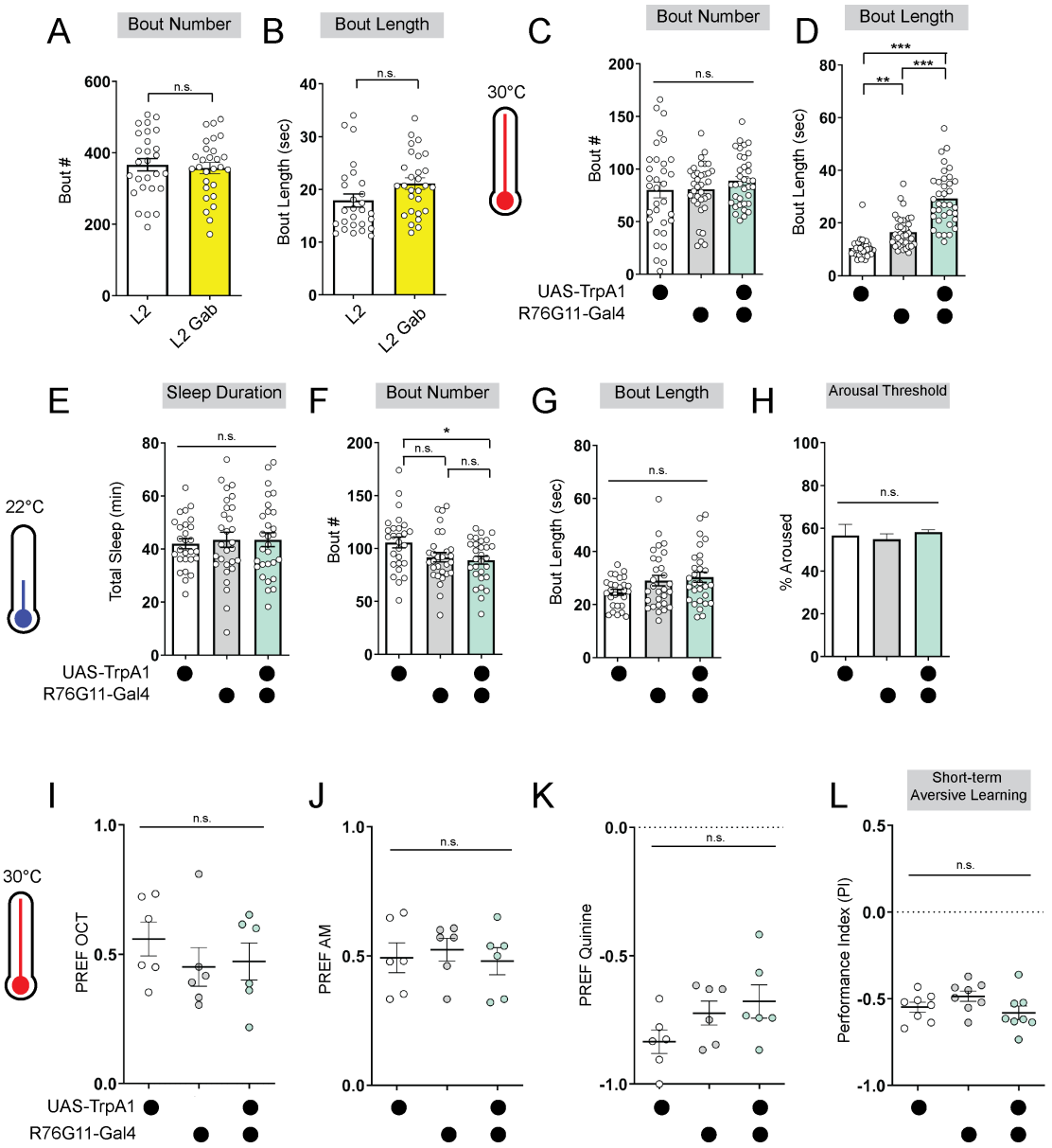

Supplemental Figure 3: Baseline sleep and odor preferences are not disrupted by *R76G11*-Gal4 manipulations.

(A, B) Sleep bout number (A) and bout length (B) of L2 control fed vehicle control (L2) or Gaboxadol (L2 Gab). **(C, D)** Sleep bout number (C) and bout length (D) of L2 expressing *R76G11*-Gal4>*UAS-TrpA1* and genetic controls at 30°C. **(E-H)** Sleep duration (E), bout number (F), bout length (G), and arousal threshold (H) of L2 expressing *R76G11*-Gal4>*UAS-TrpA1* and genetic controls at 22°C (temperature controls). **(I-K)** Naïve OCT, AM, and quinine preference in L2 expressing *R76G11*-Gal4>*UAS-TrpA1* and genetic controls at 30°C. **(L)** Short-term aversive memory performance of L2 expressing *R76G11*-Gal4>*UAS-TrpA1* and genetic controls at 30°C. A, B, n=28 larvae; C-D, n=33-36 larvae; E-G, n=27-29 larvae; H, n=145-316 sleep episodes, 30-40 larvae per genotype; I-K, n=6 PREFs (180 larvae) per genotype; L, n=8

PIs (240 larvae) per genotype. Unpaired two-tailed Student's *t*-tests [(A-B)]; One-way ANOVAs followed by Sidak's multiple comparisons tests [(C-L)].

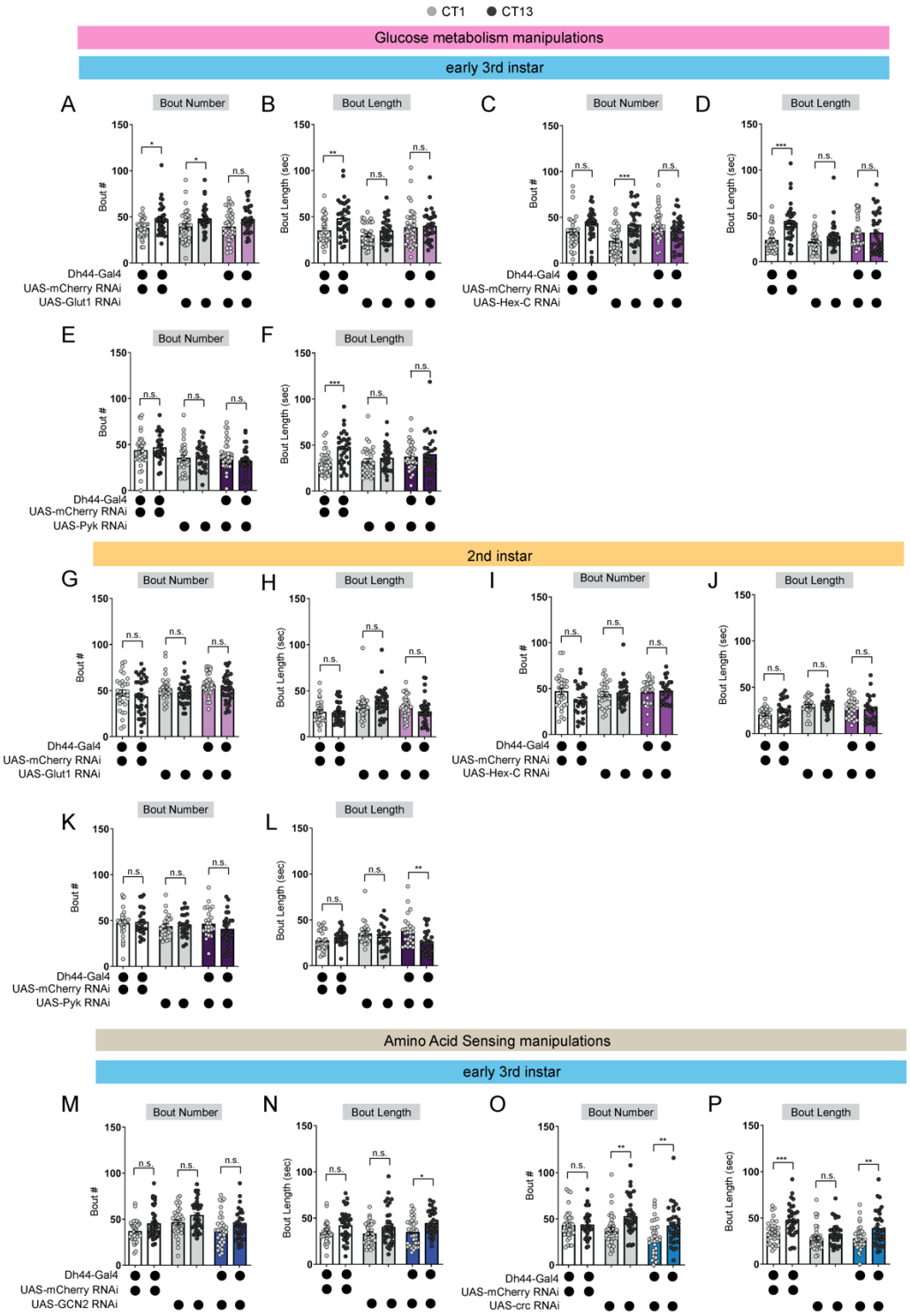

Supplemental Figure 4: Glucose metabolic gene manipulations affect L3 sleep. (A, B) Sleep bout number (A) and bout length (B) in L3 expressing *UAS-Glut1-RNAi* with *Dh44-Gal4* and genetic controls at CT1 and CT13. **(C, D)** Sleep bout number (C) and bout length (D) in L3 expressing *UAS-Hex-C-RNAi* with *Dh44-Gal4* and genetic

controls at CT1 and CT13. **(E, F)** Sleep bout number (E) and bout length (F) in L2 expressing *UAS-Glut1-RNAi* with *Dh44-Gal4* and genetic controls at CT1 and CT13. **(G, H)** Sleep bout number (G) and bout length (H) in L2 expressing *UAS-Hex-C-RNAi* with *Dh44-Gal4* and genetic controls at CT1 and CT13. **(I, J)** Sleep bout number (I) and bout length (J) in L3 expressing *UAS-GCN2-RNAi* with *Dh44-Gal4* and genetic controls at CT1 and CT13. A-J, n=32-40 larvae. Two-way ANOVAs followed by Sidak's multiple comparison test [(A-J)].